Investigation of the mechanism of proton translocation by NADH:ubiquinone oxidoreductase (complex I) from bovine heart mitochondria: does the enzyme operate by a Q-cycle mechanism?

Steven Sherwood, Judy Hirst

Biochemical Journal Immediate Publication. Published on 8 Aug 2006 as manuscript BJ20060766

Investigation of the mechanism of proton translocation by NADH:ubiquinone oxidoreductase (complex I) from bovine heart mitochondria: does the enzyme operate by a Q-cycle mechanism ?

Steven Sherwood and Judy Hirst*

Medical Research Council Dunn Human Nutrition Unit, Wellcome Trust / MRC Building, Hills Road, Cambridge, CB2 2XY, U. K.

*Author to whom correspondence should be addressed:
Medical Research Council Dunn Human Nutrition Unit, Wellcome Trust / MRC Building, Hills Road, Cambridge, CB2 2XY, U. K.
Tel : +44 1223 252810, Fax : +44 1223 252815, E-mail : jh@mrc-dunn.cam.ac.uk

Keywords:
Electron transport chain; Complex I; NADH:ubiquinone oxidoreductase; Q cycle mechanism; Reductant induced oxidation; Respiratory chain.

Running title:
'Investigation of a Q-cycle mechanism in complex I'

Abbreviations used:
CI, complex I; CHAPS, 3-[(3-cholamidopropyl) dimethylammonio]-1-propane-sulphonate; DDM, n-dodecyl-β-D-maltopyranoside; DQ, decylubiquinone; FeS, iron-sulphur cluster; FMN, flavin mononucleotide; LSQ, least-squares error value; Q_2, ubiquinone with two isoprenoid units; Q, ubiquinone; QH_2, ubiquinol; SQ, semiquinone; SMP, submitochondrial particle.

SYNOPSIS

NADH:ubiquinone oxidoreductase (complex I) is the first enzyme of the membrane bound electron transport chain in mitochondria. It conserves energy, from the reduction of ubiquinone by NADH, as a proton motive force across the inner membrane, but the mechanism of energy transduction is not known. The structure of the hydrophilic arm of thermophilic complex I supports the idea that proton translocation is driven at (or close to) the point of quinone reduction, rather than at the point of NADH oxidation, with a chain of iron-sulphur clusters transferring electrons between the two active sites. Here we describe experiments to determine whether complex I, isolated from bovine heart mitochondria, operates via a Q-cycle mechanism analogous to that observed in the cytochrome bc_1 complex. No evidence for the 'reductant-induced oxidation' of ubiquinol could be detected – therefore, no support for a Q-cycle mechanism was obtained. Unexpectedly, in the presence of NADH, complex I inhibited by either rotenone or piericidin A was found to catalyse the exchange of redox states between different quinone and quinol species, providing a possible route for future investigations into the mechanism of energy transduction.

INTRODUCTION

NADH:ubiquinone oxidoreductase (complex I) is the first enzyme of the membrane bound electron transport chain in mitochondria [1, 2]. It oxidizes NADH, produced predominantly by the tricarboxylic acid cycle in the mitochondrial matrix, and reduces ubiquinone in the inner mitochondrial membrane. The ubiquinol is reoxidised by the cytochrome bc_1 complex and the electrons are used ultimately to reduce oxygen. In addition, complex I conserves energy as a proton motive force across the inner mitochondrial membrane, supporting ATP synthesis.

Complex I from bovine heart mitochondria has a molecular mass of approximately 1 MDa and comprises 46 different subunits [3, 4]. It has an L-shaped structure, with one arm in the membrane plane and the other extending into the mitochondrial matrix (Scheme 1A) [5]. The hydrophilic arm contains the active site for NADH oxidation (containing a flavin mononucleotide (FMN)), and eight iron-sulphur clusters, two [2Fe-2S] clusters and six [4Fe-4S] clusters [6, 7]. In the bovine enzyme the hydrophilic arm contains at least 14 subunits, and seven of them are conserved throughout all known complexes I [3, 4]. Recently, a structural model of the hydrophilic arm of complex I from *Thermus thermophilus*, containing homologues to these seven subunits, has been reported, confirming that the clusters form a chain between the FMN and the ubiquinone binding site [6].

Many varied reaction mechanisms have been proposed for proton translocation by complex I (see, for recent reviews, [8-10]). However, the structure of the hydrophilic arm [6] supports the notion that proton translocation is driven at (or close to) the point of quinone reduction. The iron-sulphur clusters are likely to act predominantly as innocent electron carriers, although the final cluster in the chain, cluster N2, is close to the putative quinone binding site and may play a more intimate role in catalysis. Consequently, realistic mechanistic proposals for energy transduction by complex I fall into three categories – directly coupled proton translocation (as observed in cytochrome *c* oxidase [11]), indirectly coupled proton translocation (proton transfer is driven by (or drives) a reaction at a remote site, as in ATP synthesis [12, 13]), and Q-cycle mechanisms (as in the cytochrome bc_1 complex [14, 15]). Here, we aim to determine whether complex I operates by a Q-cycle-type mechanism.

Various Q-cycle mechanisms have been proposed previously for catalysis by complex I [16, 17]. We focus on the elegant but simple proposal of Dutton and coworkers [17], that the Q-

cycle mechanism in complex I is the 'mirror-image' of that established for the cytochrome bc_1 complex. Because a direct analogy of the mechanism of the bc_1 complex alone can account for only two of the four protons which are pumped by complex I for every NADH oxidized, an additional 'proton-pumping' component was incorporated into Dutton's mechanism [17]. The strategy adopted here does not address this component. A number of experimental observations are consistent with a Q-cycle in complex I, including evidence for more than one Q-binding site [18], and observations of semiquinone intermediates, at least one of which responds to the proton motive force [19]. However, no bound cofactor has yet been identified in the membrane domain of complex I to mediate electron transfer between two Q-sites located on opposite sides of the membrane, and evidence has been presented also which challenges proposals for more than one Q-binding site [20].

Here, we describe experiments designed to test whether a Q-cycle mechanism can be detected in complex I from bovine mitochondria. The principle of our experiment is to ask whether 'reductant-induced oxidation' of ubiquinol occurs during catalysis. Thus, our experiment is inspired by the transient increase in reduction of the *b*-haems in the cytochrome bc_1 complex, observed by Chance upon a pulse of oxygen to slowly respiring mitochondria [21], which led to development of the modified Q-cycle mechanism [14]. In the bc_1 complex the status of the individual cofactors can be defined spectroscopically, but the poor spectroscopic signals of the cofactors in complex I (flavin, iron-sulphur clusters and quinones) preclude this option. Consequently, our experiments are aimed at detecting the oxidation of ubiquinol, induced by the reduction of complex I by NADH.

EXPERIMENTAL

Preparation of complex I from bovine mitochondria

Mitochondria were isolated from bovine hearts and used to prepare mitochondrial membranes [22, 23]. Complex I was purified as described previously [24], at 4 °C, with minor modifications. 30 ml of membranes (protein ~12 mg ml^{-1}) were solubilised with 1 % n-dodecyl-β-D-maltopyranoside (DDM, Anatrace) for 30 min. in the presence of 2 mM dithiothreitol (DTT, Melford Laboratories) and 0.005 % phenylmethylsulphonyl fluoride (PMSF, Sigma), and

centrifuged (30 min., 48,000 g). The supernatant was loaded onto a 70 ml Q-Sepharose column (Amersham Pharmacia Biotech), equilibrated with buffer A (20 mM Tris-HCl, 2 mM EDTA, 0.1 % DDM, 0.005 % asolectin (Fluka, partially repurified by washing with acetone [25]) and 10 % ethylene glycol, pH 8) and eluted using a NaCl gradient. Complex I containing fractions were pooled, concentrated in a Vivaspin concentrator (100 kDa cut-off), applied to a Sephacryl S-300 gel filtration column (Amersham Pharmacia Biotech) and eluted in 20 mM sodium phosphate, 150 mM NaCl, 0.1 % DDM, 10 % glycerol and 0.1 mM tris(carboxyethyl) phosphine (TCEP, Sigma), pH 7.5. Complex I containing fractions were pooled, concentrated, and stored in liquid nitrogen.

Assays of the NADH:ubiquinone oxidoreductase activity

Complex I (2 μl of 10 – 20 mg ml^{-1}) was placed in the bottom of a cuvette, and mixed with 40 μl of 1 % asolectin (solubilised in 1 % 3-[(3-cholamidopropyl) dimethylammonio]-1-propane-sulphonate (CHAPS, Calbiochem)). 938 μl of assay buffer (20 mM potassium phosphate pH 7.5 at 30 °C) and 100 μM NADH (Sigma, 10 μl of a 10 mM solution) were added, and the solution was mixed and incubated at 30 °C for two minutes to remove a 'lag phase', attributed to a deactive form of the enzyme [26, 27]. The assay was initiated by addition of 100 μM DQ or Q_2 (Sigma, 10 μl of a 10 mM solution in ethanol) and NADH oxidation was monitored spectrophotometrically (340 – 380 nm, $\varepsilon = 4.8$ mM^{-1} cm^{-1}).

Preparation and storage of DQH_2 and Q_2H_2

DQH_2 and Q_2H_2 were prepared in an anaerobic glovebox (Belle Technology, $O_2 < 2$ ppm) [28]. Approximately 2 mg of DQ or Q_2 were dissolved in 1 ml of diethyl ether, then 2 ml of sodium dithionite (2.3 mM in 1 M potassium phosphate, pH 7) was added and the mixture shaken vigorously. The aqueous and organic phases were allowed to separate, the bottom aqueous layer was discarded, and the process repeated. The colourless organic phase was then washed twice with a saturated NaCl solution containing 10 mM HCl, and passed through a small column of anhydrous sodium sulphate. The diethyl ether was removed by evaporation and the resulting powder redissolved in ethanol containing 6 mM HCl. The final quinol concentration was determined spectrophotometrically or by HPLC analysis, which showed that typically 2-5 % of the quinone remains oxidized. The quinols could be stored anaerobically in acidified ethanol at

– 20 °C, and HPLC analysis demonstrated less than 1 % reoxidation after a week. However, after an hour exposure to air, 17 % reoxidation was observed. Consequently, all experiments involving quinols were carried out in the anaerobic glovebox. HPLC experiments carried out at varying flow rates confirmed that quinol reoxidation during the HPLC run is negligible.

Reverse phase HPLC separation and quantification of Q and QH_2 species

HPLC analysis was carried out using an Agilent 1100 series HPLC system equipped with a manual injector (Rheodyne injection valve), column thermostat (30 ºC) and multiple wavelength detector, and controlled by an Agilent ChemStation. DQ, DQH_2, Q_2 and Q_2H_2 were eluted from a Nucleosil C18 column (5 μm, 25 cm x 3.2 mm, Hichrom) in a mobile phase of 50 mM sodium perchlorate in 53:25:22:0.1 v/v/v/v ethanol / water / methanol / 70 % perchloric acid, with detection at 278 and 290 nm (adapted from a published protocol [29]). All solvents were HPLC grade (Sigma) and water was from a MilliQ purification system. The four Q species were separated at 0.4 ml min^{-1} during a run time of 40 minutes, and elute at ~8.2 min. (Q_2H_2), ~12.0 min. (Q_2), ~14.5 min. (DQH_2) and ~23.0 min. (DQ). The extinction coefficients are discussed below and reported in Table 1. Standard solutions were prepared in the HPLC mobile phase at concentrations between 0 and 100 μM.

Preparation of samples for HPLC analysis

Complex I (24 μl of 10 – 20 mg ml^{-1}) was placed in the bottom of a glass vial and mixed with either 30 μl of 1 % bovine heart polar phospholipids (Avanti Polar Lipids) or 45 μl of 1 % asolectin (solubilised in 2 or 1 % CHAPS respectively). ~2850 μl (calculated for a final volume of 3 ml) of 10 mM HEPES buffer (pD 7.5 in D_2O, 30 °C) and 100 μM NADH (30 μl from a 10 mM stock solution) were added, and the solution was mixed and incubated for two minutes whilst stirring slowly. The reaction was initiated by addition of the appropriate Q species to a final concentration of approximately 100 μM (60 μl of a 50 x concentrated stock solution in acidified ethanol). Aliquots of 100 μl were removed at set time points, and added to 300 μl of quenching solution (53:22 v/v ethanol/methanol), allowing analysis by HPLC without further manipulation. HPLC analysis confirmed that this procedure quenched all reactions efficiently. The samples were sealed anaerobically, frozen, and stored in liquid nitrogen. For analysis, they were removed one at a time from the liquid nitrogen, thawed, filtered using a 0.2 μm filter

(Sartorius Minisart RC 4), and loaded into the injection syringe (all procedures in the glove box), then injected quickly onto the HPLC column. The NADH concentration of each aliquot was determined by UV-visible spectroscopy (340 nm, $\varepsilon = 6.37\ cm^{-1}\ mM^{-1}$ in this solvent mixture).

Data modelling calculations

Data sets from HPLC analysis were fit by minimizing the least squares error value (LSQ) between calculated curves and experimental data sets. The initial concentration of each Q species was allowed to vary within a small range to account for experimental error, and rate constants were defined by calculating curves for a wide range of possible values, then refining the best fit values. Analytical solutions describing concentration as a function of time were used when possible. Otherwise, digital step calculations were used. Digital simulations use rate equations to calculate small changes in concentration which occur upon small steps in time - when decreasing the step size does not alter the results the simulation has converged to the analogue solution.

RESULTS AND DISCUSSION

Experimental strategy

Scheme 1A depicts complex I in the inner-mitochondrial membrane, catalysing the oxidation of NADH coupled to the reduction of ubiquinone and to proton translocation. The mechanism of proton translocation is not defined. Scheme 1B illustrates one possible mechanism: complex I catalysing by a modified Q-cycle mechanism analogous to that employed by the cytochrome bc_1 complex [17]. Quinone (Q) binds at the matrix side of the membrane and is reduced by two electrons, one from the iron-sulphur clusters (derived from NADH) and the other from a quinol (QH_2) bound on the outside membrane face. This step is the reverse of the bifurcation reaction in the bc_1 complex [14, 15] and it leads to a bound semiquinone on the outside face - which is oxidized completely upon reduction of a second quinone. Thus, oxidation of one NADH is coupled to the reduction of two quinones and to the oxidation of one quinol, with spatial separation of the redox processes providing net proton translocation. The experimental strategy applied here is to provide complex I with different (distinguishable) species of Q and QH_2, and to

ask whether any QH_2 is oxidized during catalysis (see Figure 1). Directly or indirectly (conformationally) coupled mechanisms of proton translocation should not lead to 'reductant induced oxidation' (Figure 1A), whereas a Q-cycle mechanism should result in the oxidation of one QH_2 for every NADH oxidized (Figure 1B).

Key requirements for the success of our strategy are: i) the availability of two quinone species with similar physical and catalytic properties; ii) a method of accurately quantifying the four quinone/ol species present; iii) the absence of significant alternative routes for the oxidation of QH_2. Decylubiquinone (DQ) and ubiquinone-2 (Q_2) both contain 10-carbon sidechains and have similar physical properties [30, 31]. The reactions of both of them with complex I have been studied [31-36], and the general picture is that they are both reduced by complex I in an inhibitor-sensitive manner, and their reduction is coupled to proton translocation. However, differences in their catalytic properties have been observed, notably Q_2 supports a lower rate of turnover than DQ [31, 33, 35], and Q_2 shows a greater tendency than DQ to react at the 'inhibitor-insensitive site' on complex I, commensurate with its higher hydrophilicity [33]. Here we have taken these differences into account by, first, quantifying the behaviour of both quinones under the conditions used here (Scheme 2A), and second, by carrying out all experiments in duplicate (interchanging the identities of each of the quinone / quinol species) to balance out any variations. Importantly, both oxidation states of DQ and Q_2 are readily distinguished and quantified by HPLC analysis (see below). The main obstacle to our strategy was found to be the 'self-exchange reaction' between Q and QH_2 (Scheme 2B) [28], which exchanges the redox states of the two species and provides an alternative route for QH_2 oxidation. This reaction precluded an end-point or 'pulse' approach (taking catalytic turnover to completion with varying amounts of NADH), and required catalysis to be analysed during an experimental timecourse. However, the exchange reaction could be quantified accurately according to a simple bimolecular reaction (Scheme 2B) thus, providing that its rate is not prohibitively fast, it can be readily factored into simulations of experimental data.

Quantification of DQ, Q_2, DQH_2 and Q_2H_2 by HPLC

The reverse phase HPLC method was capable of separating and quantifying all four species in a single experiment (see Figure 2). For each species, peak area was directly proportional to the concentration loaded onto the column, and determinations of the concentration of an unknown

sample were reproducible (multiple injections gave values which differed by less than 1 %), with a limit of quantification of ~1 μM.

Accurate values of extinction coefficients in the HPLC mobile phase and in ethanol were determined as follows. The UV-visible spectra of stock solutions of DQ and Q_2 were recorded over a range of dilutions. Then, complex I was used to catalyse the reaction between NADH (0 to 100 μM) and different estimated concentrations of DQ or Q_2 (0 – 100 μM) under standard assay conditions. The reaction was incubated until no further NADH oxidation was observed (~ 10 min.), and the total amount of NADH oxidised was calculated. HPLC analysis confirmed that when [NADH] > [Q] only negligible quinone remained (< 2 μM). The amount of DQ or Q_2 present in the stock solution was calculated and the extinction coefficient determined. Each determination was carried out at least three times, and the values found agree well with published values [28, 31, 33, 37] (see Table 1). Corresponding values for the quinols were calculated by an analogous method: upon reaction with NADH the decrease in quinone concentration is equal to the increase in quinol concentration, so that comparison of the HPLC peak areas from sets of experiments from the same stock solution defined the ratio of the extinction coefficients (see Table 1). Comparison with previously reported values shows good agreement for DQH_2 [28, 38] but significant discrepancy with the single reported value for Q_2H_2 [39]. However, this published value is not consistent with reported values from other quinols. All data reported below have been calculated using the extinction coefficients determined as described above.

Development of a protocol for preparing samples for HPLC analysis

The quinone-quinol self-exchange reaction (Scheme 2B) is slow relative to enzyme turnover, but fast enough to perturb the reaction mixture significantly after a 10 min. incubation. Because it occurs in water, but not significantly in ethanol or methanol, a range of conditions were investigated in an attempt to minimize its rate. A mixture of Q_2 and DQH_2 was incubated for 10 min. at 30 °C in various test solutions, then evaluated by HPLC. Exchange is slower at lower pH (6.0 < 7.5 < 9.0, consistent with results described previously for plastoquinol-1 and ubiquinone-1 [28]), slower in D_2O than in H_2O (at equivalent pL), and accelerated by phospholipids. Different types and amounts of detergent, ethylene glycol, the ionic strength [28], and the order in which the different reagents (buffer, phospholipid and quinones) were added exerted no significant effect. However, the relative rates (exchange versus catalysis) are most important here, and

catalysis is retarded significantly in the absence of phospholipids [24], and at pH 6.0 or 9.0 relative to 7.5 - whereas exchanging H_2O for D_2O had little effect. Therefore, the chosen conditions were 0.1 mg ml^{-1} of bovine heart phospholipids or 0.15 mg ml^{-1} asolectin (decreased below the optimal 'catalytic' level to minimise the exchange reaction), in D_2O, at pD = 7.5 and 30 °C. The enzyme was incubated for 2 min. in the presence of 100 μM NADH before the reaction was initiated with the Q / QH_2 mixture. Finally, quenching the reaction with a 3-fold excess of ethanol / methanol (53:22 v / v) rapidly stopped both catalysis and exchange and allowed storage and anaerobic freeze / thawing without alteration in composition. In addition, the quenched mixture could be injected directly onto the HPLC column, and NADH in the solution was stable, allowing its analysis by UV-visible spectroscopy.

The reduction of DQ and Q_2 by NADH and validation of the experimental approach

In catalytic activity assays variation in the initial rate of NADH oxidation as a function of the concentrations of DQ and Q_2 defines apparent values for K_M and k_{cat} (in applying the Michaelis-Menten equation no assumption about the actual mechanism is intended). Values of K_M and k_{cat} derived here are reported in Table 2, and compared with published values. First, the K_M values are significantly higher than values derived using submitochondrial particles (SMPs) [31, 40], but not necessarily higher than the values of Hano and coworkers derived using isolated complex I [35]. K_M is known to depend strongly on the hydrophobic phase volume [31], as the concentration of quinone in the hydrophobic phase is much higher than the average concentration in the cuvette. Previously, Fato and coworkers calculated 'true' K_M values of 120 - 138 mM for DQ and 11.5 - 36 mM for Q_2 [31], the K_M for endogenous Q_{10} is in the mM range in membrane lipids [41], and values recorded here varied according to phospholipid concentration. Thus, the smaller values determined using SMPs probably correspond to small hydrophobic phase volumes. Second, k_{cat} values of 3.1 (DQ) and 1.8 (Q_2) μmol min^{-1} mg^{-1} were typical under the conditions employed in generating samples for HPLC analysis, though, as expected, they are slightly lower than corresponding values recorded previously [24] because of the decreased phospholipid concentration in the assay buffer. As expected, k_{cat} is smaller for Q_2 than for DQ, and although the absolute rates differ between preparations, good agreement in $k_{cat}DQ/k_{cat}Q_2$ is found throughout Table 2. All catalytic rates described here are >90 % sensitive to inhibition by

rotenone or piericidin A (the sensitivity of DQ is higher than that of Q_2, as described previously [33]).

In significant quinol concentrations the characteristics of product inhibition should also be defined. Product inhibition in complex I is poorly understood. Ohshima and coworkers suggested that quinols are competitive inhibitors, and showed that 40 μM Q_2H_2 was sufficient to inhibit Q_1 reduction in SMPs completely [40]. However, for other combinations of Q and QH_2 only 40 % inhibition could be attained, incompatible with a simple competitive inhibition model. Later, Nakashima and coworkers suggested that Q_1H_2 is a competitive inhibitor of Q_1 reduction, but no kinetic parameters were reported [42]. In fact, it would be surprising if quinol inhibition did conform to any simple pattern. For example, the relative binding affinities of Q and QH_2 are likely to depend on the oxidation states of the enzyme's redox cofactors and so to depend on the relative rates of NADH oxidation and Q reduction - and complex I may adopt multiple conformations during the proton pumping cycle also. In addition, appropriate experiments are technically difficult (for example, quinols are sensitive to O_2) and difficult to interpret (for example, because of differences in the solubility and partition coefficients of the reactant and product species). In the experiments described here we found that a naive competitive inhibition model (Scheme 2A) was able to reproduce measured data satisfactorily, though it is unlikely to reflect the actual mechanism. Thus, sets of ten assay traces, covering a range of initial DQ and DQH_2 (or Q_2 and Q_2H_2) concentrations, were recorded and modelled according to Scheme 2A, using the corresponding equation in Table 3 and the K_M values in Table 2. Then, effective values for $K_{I(DQH2)}$ and $K_{I(Q2H2)}$ were estimated by optimising the fit between the model and the data (Table 2).

Figure 3 shows how the reduction of a single quinone species (DQ or Q_2), by complex I and NADH, could be monitored accurately using HPLC and modelled using Scheme 2A and the values reported in Table 2. In Scheme 2A the rate is controlled completely by quinone reduction, not NADH oxidation, because NADH:ferricyanide or hexaammine ruthenium oxidoreduction by complex I is significantly faster than NADH:ubiquinone oxidoreduction [26, 43, 44], showing that NADH oxidation is not rate limiting. Figure 3 validates Scheme 2A and our experimental approach because: i) the total amount of quinone species (Q + QH_2) calculated using the extinction coefficients reported in Table 1 remains constant throughout; ii) the decrease in NADH concentration matches the decrease in the quinone concentration and the increase in the quinol

concentration; iii) agreement between the experimentally recorded data and the model is excellent, and the errors in each data point are small.

Quantitative characterization of the exchange reaction

Figure 4 shows data from HPLC analysis of the exchange reaction. In all cases the total amounts of each species {DQ + DQH_2} and {Q_2 + Q_2H_2}, and of each oxidation state {DQ + Q_2} and {DQH_2 + Q_2H_2} remain constant throughout. Scheme 2B shows the reaction mechanism used to model the data, a bimolecular reaction between quinol and quinone, where k_1 refers to both the forward and backward reactions [28]. Figure 4 shows clearly that the equation derived from Scheme 2B (see Table 3) describes the experimental data accurately. Only slight improvements (typically the LSQ value decreases by ~5 %) resulted from letting the forward and backward rate constants differ. The measured exchange rate constants are summarized in Table 4, demonstrating that the rate constant does not depend on the combination of quinones used (rows 1 and 2 vs. 3 and 4), or on the presence of NADH, complex I, or inhibitor alone (rows 1 to 4), but that it is larger in the presence of bovine phospholipids than asolectin phospholipids (rows 1 and 3 vs. 2 and 4).

Reactions to quantify the self-exchange reaction were also carried out in the presence of all the components of the assay (buffer, phospholipids, complex I, NADH, Q and QH_2) but with a complex I inhibitor (rotenone or piericidin A) present (see Figure 5). Complex I is thought to reduce quinone at two different sites: the 'inhibitor sensitive site' is associated with hydrophobic quinone substrates and proton translocation, while the 'inhibitor insensitive site' accepts more hydrophilic substrates and is decoupled from the proton-motive force [33, 45-47]. The two substrates used here, DQ and Q_2, display a small component of inhibitor insensitive activity, so that the inhibited enzyme exhibits a slow rate of ubiquinone reduction. Quinone substrates with higher hydrophobicity (to increase the inhibitor sensitivity) are precluded by their insolubility in aqueous buffers [31-34]. Figure 5 shows three typical data sets, and the data fits obtained using Scheme 2B in conjunction with Scheme 2C to describe the inhibitor insensitive reduction (see Table 3). The agreement between the data and the model is excellent, and Table 4 includes the rate constants derived for the exchange reaction. Unexpectedly, the exchange reaction is accelerated significantly in the presence of inhibited complex I (all the substrates are present and turnover is actively inhibited). Because the inhibitor insensitive reaction is not associated with

proton translocation [33] the increased exchange rate is unlikely to be associated with energy transduction. Possible explanations are discussed below.

Catalysis of NADH:ubiquinone oxidoreduction in the presence of ubiquinol

Figure 6 shows two data sets from the complex I catalysed reduction of either DQ or Q_2, in the presence of Q_2H_2 or DQH_2 respectively. In each case the total amount of each Q-species remains constant throughout the assay, and the decrease in the total quinone concentration is equal to the increase in the total quinol concentration, and to the decrease in the concentration of NADH. Therefore, both data sets are internally consistent. On first sight it is obvious that Figure 6 resembles Figure 1B, rather than Figure 1A, indicating the operation of a Q-cycle mechanism. However, as described below, the transient quinol oxidation may be explained *quantitatively* by the combination of the model of Figure 1A with the known rate of the self-exchange reaction. Consequently, our experiments do not provide any evidence for the operation of a Q-cycle mechanism in complex I.

It is immediately apparent, from the relative rates of NADH oxidation and quinone reduction, that Q_2H_2 slows the reduction of DQ severely, and that DQH_2 slows the reduction of Q_2 also. The relative effects of Q_2H_2 and DQH_2 in this 'cross-over' reaction were confirmed in solution assays, but are only qualitatively consistent with the values of K_M, k_{cat} and K_I reported in Table 2 (calculated according to Scheme 2D and the corresponding equations in Table 3). It is likely that Scheme 2D is not a sufficient (or correct) description of the mechanism. Consequently, instead of attempting to apply Scheme 2D to the data shown in Figure 6, a pragmatic approach (avoiding any definition of the characteristics of product inhibition) was adopted as follows. The NADH concentration, at a given time, defines the total amount of quinone which has been reduced. Thus, changes in the individual quinone and quinol concentrations can be estimated from the amount of NADH oxidised, provided that the 'preference' of the enzyme to react with either DQ or Q_2 is known. First, calculations using Scheme 2D and the K_M and k_{cat} values given in Table 2 suggest that complex I should display a slight preference for DQ. For example, in the presence of 50 μM DQ and 50 μM Q_2, DQ reduction is expected to account for 59 % (not 50 %) of the overall reduction rate. 50 μM DQ and 50 μM Q_2 is the point (in a total concentration of 100 μM Q) at which complex I is predicted to deviate most from a 'chance encounter' model, in which the enzyme reacts simply according

to the concentration of the different species which are present (for example, in 70 μM DQ and 30 μM Q_2 DQ reduction would account for 70 % of the overall rate). Subsequently, experiments employing HPLC to analyse a range of DQ and Q_2 concentrations suggested that the chance encounter model actually provides an accurate picture, with very little deviation found in any case (the ratio of (DQ reduced / total reduction) to (DQ concentration / total concentration) varied only from 0.95 to 1.05). Therefore, the simple chance encounter model was applied to model the data presented in Figure 6. Future investigations, using a wider range of quinones, may help to define whether the chance encounter model reflects the catalytic mechanism, or whether its accuracy, in this case, results simply from the similarity in the apparent K_M and k_{cat} values (Table 2).

Figure 7 shows that excellent agreement with the experimental data is obtained by using the chance encounter model in combination with measured changes in NADH concentration. The fits in Figure 7 rely on only a single variable, the exchange rate constant (k_1 in Table 3), and derived values from different data sets lie between 40 and 75 mol^{-1} dm^3 s^{-1}. Thus, the data reported in Figure 7 can be explained without using a Q-cycle mechanism, and by using an exchange rate constant equivalent to values measured in the presence of inhibited complex I (see Table 4). Clearly, this is evidence against the operation of a Q-cycle mechanism. However, the exchange rate constants required to fit the data are those from the inhibited enzyme (complex I + NADH + inhibitor), and they are significantly larger than equivalent values from complex I alone, NADH alone, or complex I + inhibitor in the absence of NADH. Two features are common to the inhibited complex I and to complex I during turnover. i). The flavin and the iron-sulphur clusters are reduced in each case (NADH oxidation is much faster than Q reduction during catalysis). ii). The slow, inhibitor insensitive reaction occurs in both cases. If the reduced, inhibited enzyme facilitates the self-exchange reaction then it may reflect the existence of a alternative conformation, or a state in which the environment of one or more redox-active centres is altered. However, it is perhaps more likely that the inhibitor insensitive reaction increases exchange via the formation of semiquinone intermediates. Interestingly, redox equilibration between duroquinol and Q_2 has been reported to be catalysed by the cytochrome bc_1 complex also [48]. The reaction proceeds by reduction of cofactors in the enzyme by duroquinol, followed by the reduction of Q_2 to Q_2H_2. However, it is unlikely that complex I catalyses the reaction by this mechanism as the oxidised enzyme does not increase the exchange rate, and

because Q_2H_2 and DQH_2 have much higher potentials than any of the known complex I cofactors. As expected, no evidence for any reduced FeS clusters was observed by EPR when DQH_2 or Q_2H_2 were used to attempt to reduce complex I, irrespective of whether an inhibitor was present or not.

Finally, note that the experimental data can also be fit reasonably well by using an analogous approach, but with a mechanism that comprises the reaction of two quinones and one quinol, again using a chance-encounter model. However, the fits are compromised because data sets acquired using DQ and Q_2H_2 can be fit well only if the rate of exchange is zero (with the best fits using slightly negative values) and because those acquired using Q_2 and DQH_2 show systematic errors with LSQ values several times higher than provided by the simple model. Consequently, although our data do not support a Q-cycle mechanism in complex I, we must accept that the increased rate of the exchange reaction observed during turnover and with the inhibited enzyme (observations which are worthy of future investigation) compromises the certainty of our conclusion.

Implications for the mechanism of complex I

The experiments described here provide no support for the operation of a Q-cycle mechanism in complex I, and all data can be explained accurately by the 'simple' reduction of Q to QH_2. However, our data do not exclude a Q-cycle mechanism unambiguously. First, the increased rate of Q / QH_2 exchange, catalysed by the inhibited enzyme and proposed to occur also during turnover, remains unexplained and is worthy of future consideration. We believe that it does not indicate a Q-cycle mechanism because 'inhibitor insensitive' catalysis is not coupled to the proton motive force. Second, we cannot exclude the possibility that Q, generated from QH_2, is retained in the vicinity of the 'reducing' active site, promoting its immediate re-reduction and so precluding its detection. Most simply, Q could be released from the enzyme at a point which is close to the entry to the Q-binding site (at present no information on the spatial arrangement of the Q-binding sites in complex I exists). An additional possibility is that Q is retained in the enzyme and 'switched' internally to the second active site, requiring controlled directional uptake and release of protons from a single large site to alternate sides of the membrane. A semiquinone 'switch' mechanism has been proposed previously, conforming to this suggestion [49]. Finally, if complex I does not catalyse by a Q-cycle type mechanism then it is likely to translocate protons

either by direct coupling at cluster N2 or at the site of quinone reduction, or to use a conformational change mechanism (see, for recent reviews, [8-10]). Clearly, determination of the mechanism of energy transduction by this complicated enzyme will require new structural information and creative approaches to functional studies of catalysis.

ACKNOWLEDGEMENTS

This work was supported by The Medical Research Council.

REFERENCES

1 Schultz, B. E. and Chan, S. I. (2001) Structures and proton-pumping strategies of mitochondrial respiratory enzymes. Annu. Rev. Biophys. Biomol. Struct. **30**, 23-65

2 Saraste, M. (1999) Oxidative phosphorylation at the *fin de siècle*. Science **283**, 1488-1493

3 Hirst, J., Carroll, J., Fearnley, I. M., Shannon, R. J. and Walker, J. E. (2003) The nuclear encoded subunits of complex I from bovine heart mitochondria. Biochim. Biophys. Acta **1604**, 135-150

4 Walker, J. E. (1992) The NADH-ubiquinone oxidoreductase (complex I) of respiratory chains. Q. Rev. Biophys. **25**, 253-324

5 Hofhaus, G., Weiss, H. and Leonard, K. (1991) Electron-microscopic analysis of the peripheral and membrane parts of mitochondrial NADH dehydrogenase (complex I). J. Mol. Biol. **221**, 1027-1043

6 Sazanov, L. A. and Hinchliffe, P. (2006) Structure of the hydrophilic domain of respiratory complex I from *Thermus thermophilus*. Science **311**, 1430-1436

7 Ohnishi, T. (1998) Iron-sulphur clusters / semiquinones in complex I. Biochim. Biophys. Acta **1364**, 186-206

8 Brandt, U., Kerscher, S., Dröse, S., Zwicker, K. and Zickermann, V. (2003) Proton pumping by NADH:ubiquinone oxidoreductase. A redox driven conformational change mechanism? FEBS Lett. **545**, 9-17

9 Hirst, J. (2005) Energy transduction by respiratory complex I - an evaluation of current knowledge. Biochem. Soc. Trans., **33**, 525-529

10 Yagi, T. and Matsuno-Yagi, A. (2003) The proton-translocating NADH-quinone oxidoreductase in the respiratory chain: the secret unlocked. Biochemistry **42**, 2266-2274

11 Belevich, I., Verkhovsky, M. I. and Wikström, M. (2006) Proton-coupled electron transfer drives the proton pump of cytochrome *c* oxidase Nature **440**, 829-832

12 Stock, D., Gibbons, C., Arechaga, I., Leslie, A. G. W. and Walker, J. E. (2000) The rotary mechanism of ATP synthase. Curr. Opin. Struct. Biol. **10**, 672-679

13 Toyoshima, C., Nomura, H. and Sugita, Y. (2003) Structural basis of ion pumping by Ca^{2+}-ATPase of sarcoplasmic reticulum. FEBS Lett. **555**, 106-110

14 Trumpower, B. L. (1990) The protonmotive Q cycle. J. Biol. Chem. **265**, 11409-11412

15 Berry, E. A., Guergova-Kuras, M., Huang, L.-S. and Crofts, A. R. (2000) Structure and function of cytochrome *bc* complexes. Annu. Rev. Biochem. **69**, 1005-1075

16 Brandt, U. (1997) Proton-translocation by membrane-bound NADH:ubiquinone-oxidoreductase (complex I) through redox-gated ligand conduction. Biochim. Biophys. Acta **1318**, 79-91

17 Dutton, P. L., Moser, C. C., Sled, V. D., Daldal, F. and Ohnishi, T. (1998) A reductant-induced oxidation mechanism for complex I. Biochim. Biophys. Acta **1364**, 245-257

18 Esposti, M. D. (1998) Inhibitors of NADH-ubiquinone reductase: an overview. Biochim. Biophys. Acta **1364**, 222-235

19 Magnitsky, S., Toulokhonova, L., Yano, T., Sled, V. D., Hägerhall, C., Grivennikova, V. G., Burbaev, D. S., Vinogradov, A. D. and Ohnishi, T. (2002) EPR characterisation of ubisemiquinones and iron-sulphur cluster N2, central components of the energy coupling in the NADH-ubiquinone oxidoreductase (complex I) in situ. J. Bioenerg. Biomembr. **34**, 193-208

20 Okun, J. G., Lümmen, P. and Brandt, U. (1999) Three classes of inhibitors share a common binding domain in mitochondrial complex I (NADH:ubiquinone oxidoreductase). J. Biol. Chem. **274**, 2625-2630

21 Chance, B. (1974) Coupling between cytochromes c_1, b_T and b_K, in Dynamics of energy transducing membranes, ed. Ernster, L., Estabrook, R. W. and Slater, E. C. Elsevier Scientific Publishing Company

22 Smith, A. L. (1967) Preparation, properties and conditions for assay of mitochondria: slaughterhouse material, small scale. Meth. Enzymol. **10**, 81-86

23 Walker, J. E., Skehel, J. M. and Buchanan, S. K. (1995) Structural analysis of NADH: ubiquinone oxidoreductase from bovine heart mitochondria. Meth. Enzymol. **260**, 14-34

24 Sharpley, M. S., Shannon, R. J., Draghi, F. and Hirst, J. (2006) Interactions between phospholipids and NADH:ubiquinone oxidoreductase (complex I) from bovine mitochondria. Biochemistry **45**, 241-248

25 Darley-Usmar, V. M., Capaldi, R. A., Takamiya, S., Millett, F., Wilson, M. T., Malatesta, F. and Sarti, P. (1987) Mitochondria, A Practical Approach, eds. Darley-Usmar, V. M., Rickwood, D. & Wilson, M. T. (Oxford), pp. 143-144

26 Vinogradov, A. D. (1998) Catalytic properties of the mitochondrial NADH-ubiquinone oxidoreductase (complex I) and the pseudo-reversible active / inactive enzyme transition. Biochim. Biophys. Acta **1364**, 169-185

27 Maklashina, E., Kotlyar, A. B. and Cecchini, G. (2003) Active / de-active transition of respiratory complex I in bacteria, fungi and animals. Biochim. Biophys. Acta **1606**, 95-103

28 Rich, P. R. (1981) Electron transfer reactions between quinols and quinones in aqueous and aprotic media. Biochim. Biophys. Acta **637**, 28-33

29 Takada, M., Ikenoya, S., Yuzuriha, T. and Katayama, K. (1982) Studies on reduced and oxidised coenzyme Q (ubiquinones). Biochim. Biophys. Acta **679**, 308-314

30 Rich, P. R. and Harper, R. (1990) Partition coefficients of quinones and hydroquinones and their relation to biochemical reactivity. FEBS Lett. **269**, 139-144

31 Fato, R., Estornell, E., di Bernardo, S., Pallotti, F., Castelli, G. P. and Lenaz, G. (1996) Steady-state kinetics of the reduction of coenzyme Q analogues by complex I (NADH:ubiquinone oxidoreductase) in bovine heart mitochondria and submitochondrial particles. Biochemistry **35**, 2705-2716

32 Estornell, E., Fato, R., Pallotti, F. and Lenaz, G. (1993) Assay conditions for the mitochondrial NADH:coenzyme Q oxidoreductase. FEBS Lett. **332**, 127-131

33 Degli Esposti, M., Ngo, A., McMullen, G. L., Ghelli, A., Sparla, F., Benelli, B., Ratta, M. and Linnane, A. W. (1996) The specificity of mitochondrial complex I for ubiquinones. Biochem. J. **313**, 327-334

34 Lenaz, G. (1998) Quinone specificity of complex I. Biochim. Biophys. Acta **1364**, 207-221

35 Hano, N., Nakashima, Y., Shinzawa-Itoh, K. and Yoshikawa, S. (2003) Effect of the side chain structure of coenzyme Q on the steady state kinetics of bovine heart NADH:coenzyme Q oxidoreductase. J. Bioenerg. Biomembr. **35**, 257-265

36 Sakamoto, K., Miyoshi, H., Ohshima, M., Kuwabara, K., Kano, K., Akagi, T., Mogi, T. and Iwamura, H. (1998) Role of the isoprenyl tail of ubiquinone in reaction with respiratory enzymes: studies with bovine heart mitochondrial complex I and *Escherichia coli bo*-type ubiquinol oxidase. Biochemistry **37**, 15106-15113

37 Trumpower, B. L. and Edwards, C. A. (1979) Purification of a reconstitutively active iron-sulphur protein (oxidation factor) from succinate-cytochrome *c* reductase complex of bovine heart mitochondria. J. Biol. Chem. **254**, 8697-8706

38 Ouchane, S., Agalidis, I. and Astier, C. (2002) Natural resistance to inhibitors of the ubiquinol cytochrome *c* oxidoreductase of *Rubrivivax gelatinosus*: sequence and functional analysis of the cytochrome bc_1 complex. J. Bacteriol. **184**, 3815 - 3822

39 Bennett, M. C., Mlady, G. W., Kwon, Y.-H. and Rose, G. M. (1996) J. Neurochem. **66**, 2606 - 2611

40 Ohshima, M., Miyoshi, H., Sakamoto, K., Takegami, K., Iwata, J., Kuwabara, K., Iwamura, H. and Yagi, T. (1998) Characterisation of the ubiquinone reduction site of mitochondrial complex I using bulky synthetic ubiquinones. Biochemistry **37**, 6436-6445

41 Lenaz, G., Castelli, G. P., Fato, R., D'Aurelio, M., Bovina, C., Formiggini, G., Marchetti, M., Estornell, E. and Rauchova, H. (1997) Coenzyme Q deficiency in mitochondria: kinetic saturation versus physical saturation. Molec. Aspects of Med. **18**, s25-s31

42 Nakashima, Y., Shinzawa-Itoh, K., Watanabe, K., Naoki, K., Hano, N. and Yoshikawa, S. (2002) Steady-state kinetics of NADH:coenzyme Q oxidoreductase isolated from bovine heart mitochondria. J. Bioenerg. Biomembr. **34**, 11-19

43 Ragan, C. I. (1976) NADH-ubiquinone oxidoreductase. Biochim. Biophys. Acta **456**, 249-290

44 Kussmaul, L. and Hirst, J. (2006) The mechanism of superoxide production by NADH:ubiquinone oxidoreductase (complex I) from bovine heart mitochondria. Proc. Natl. Acad. Sci. USA **103**, 7607-7612

45 Schatz, G. and Racker, E. (1966) Partial resolution of the enzymes catalysing oxidative phosphorylation. J. Biol. Chem. **241**, 1429-1438

46 Di Virgilio, F. and Azzone, G. F. (1982) Activation of site I redox-driven H^+ pump by exogenous quinones in intact mitochondria. J. Biol. Chem. **257**, 4106-4113

47 Ragan, C. I. (1978) The role of phospholipids in the reduction of ubiquinone analogues by the mitochondrial reduced nicotinamide-adenine dinucleotide-ubiquinone oxidoreductase complex. Biochem. J. **172**, 539-547

48 Marres, C. A. M. and de Vries, S. (1991) Reduction of the Q-pool by duroquinol via the two quinone-binding sites of the QH_2:cytochrome *c* oxidoreductase. A model for the equilibrium between cytochrome *b*-562 and the Q-pool. Biochim. Biophys. Acta **1057**, 51-63

49 Brandt, U. (1999) Proton translocation in the respiratory chain involving ubiquinone - a hypothetical semiquinone switch mechanism for complex I. BioFactors **9**, 95-101

TABLES

	ε in ethanol (mM^{-1} cm^{-1})		ε in mobile phase (mM^{-1} cm^{-1})	
	278 nm	**290 nm**	**278 nm**	**290 nm**
DQ	16.17 ± 1.16 {14 [28, 31]; 16 [37]; 14.5 [33]}	9.09 ± 0.54	16.63 ± 1.09	11.55 ± 0.71
Q_2	12.97 ± 1.37 {13.7 (275 nm) [31]; 14.5 [33]}	5.87 ± 0.95	12.75 ± 0.22	6.68 ± 0.34
DQH_2	-	{3.9 - 4 [28, 38]}	3.08 ± 0.43	4.10 ± 0.51
Q_2H_2	{16 (methanol) [39]}	-	2.65 ± 0.08	3.22 ± 0.32

Table 1. Extinction coefficients for the two quinone and quinol species. Extinction coefficients for DQ and Q_2 were determined in ethanol and in the HPLC mobile phase, and the values determined in ethanol are consistent with values reported previously (enclosed in {}). Extinction coefficients for DQH_2 and Q_2H_2 were determined in the HPLC mobile phase only. The value for DQH_2 matches previously reported values in ethanol but the value for Q_2H_2 does not. The error values reported are 95 % confidence intervals.

DQ K_M μM	**DQH_2 K_I** μM	**Q_2 K_M** μM	**Q_2H_2 K_I** μM	**DQ k_{cat}** μmol min^{-1} mg^{-1}	**Q_2 k_{cat}** μmol min^{-1} mg^{-1}	**k_{cat} DQ / Q_2**	**Conditions**	**Ref.**
24.0 ± 7.5	26.0 ± 10	20.4 ± 3.9	15.3 ± 4.4	3.1 ± 1.2	1.8 ± 1.0	2.5 ± 0.8	Isolated CI pH 7.5, 100 μM NADH	This work
86	-	5	-	1.85	0.55	3.4	Isolated CI pH 8.0, 5 μM NADH	[35]
6	-	2	-	0.45[1]	0.21[1]	2.1	SMPs pH 7.4, 50 μM NADH	[40]
1.8	-	1.3	-	0.58 ± 0.15[1]	0.29[1]	2.0	SMPs 75 μM NADH	[31, 34]

Table 2. Values for K_M, k_{cat} and K_I for DQ, Q_2, DQH_2 and Q_2H_2 determined in this work and compared to values reported previously. Error values are 95 % confidence intervals.
[1]Value reported per mg of total protein.

	Rate equation	Integrated rate equation
A. Catalysis - single Q with product inhibition	$\frac{dx}{dt} = \frac{k_{cat}[CI]([Q]_0 - x)}{K_M\left(1 + \frac{[QH_2]_0 + x}{K_I}\right) + ([Q]_0 - x)}$	$ax + (b + a[Q]_0)\ln\left\|\frac{[Q]_0 - x}{[Q]_0}\right\| + k_{cat}t = 0$ $a = \frac{K_M}{K_I} - 1 \quad b = K_M\left(1 + \frac{[P]_0}{K_I}\right) + [Q]_0$
B. Exchange reaction	$\frac{dx}{dt} = k_1([Q]_0 - x)([Q^*H_2]_0 - x) - k_1([QH_2]_0 + x)([Q^*]_0 + x)$	$x = \frac{([QH_2]_0[Q^*]_0 - [Q]_0[Q^*H_2]_0)(e^{-k_1 t\Sigma Q} - 1)}{\Sigma Q}$ ΣQ is the sum of the concentrations of all the Q and QH_2 species.
C. Inhibitor insensitive reaction	$\frac{dx}{dt} = k_2([Q]_0 - x)$	$x = [Q]_0\left(1 - e^{-k_2 t}\right)$
D. Catalysis - two Qs with product inhibition	$-\frac{d[DQ]}{dt}\Big)_{Q2} = \frac{k_{catDQ}K_M^{DQ}[DQ]}{\left\{1 + \frac{[DQH_2]}{K_I^{DQH_2}} + \frac{[Q_2H_2]}{K_I^{Q_2H_2}} + \frac{[DQ]}{K_M^{DQ}} + \frac{[Q_2]}{K_M^{Q_2}}\right\}}$	

Table 3. Rate equations describing the four reactions shown in Scheme 2. x is the amount of the starting material which has reacted to form products after time t and $[A]_0$ is the concentration of species A at time zero. In D) only the rate equation for the decrease in DQ at constant Q_2 concentration is given; an analogous equation is readily derived for Q_2.

Quinone species	Phospholipid	Control condition	Rate constant (mol^{-1} dm^3 s^{-1})
$DQ + Q_2H_2$	bovine	– NADH or – CI ± inhibitor	14.4 ± 4.6
$DQ + Q_2H_2$	asolectin	– NADH or – CI ± inhibitor	8.9 ± 2.6
$Q_2 + DQH_2$	bovine	– NADH or – CI ± inhibitor	18.3 ± 7.3
$Q_2 + DQH_2$	asolectin	– NADH or – CI ± inhibitor	9.1 ± 3.0
$DQ + Q_2H_2$ or $Q_2 + DQH_2$	bovine	+ NADH + CI + rotenone or piericidin A	68.0 ± 35.4
$DQ + Q_2H_2$ or $Q_2 + DQH_2$	asolectin	+ NADH + CI + rotenone or piericidin A	76.5 ± 15.7
$DQ + Q_2H_2$ or $Q_2 + DQH_2$	bovine or asolectin	+ NADH + CI + rotenone	74.8 ± 23.2
$DQ + Q_2H_2$ or $Q_2 + DQH_2$	bovine or asolectin	+ NADH + CI + piericidin A	72.3 ± 19.6

Table 4. Rate constants for the self-exchange reaction measured under different control conditions. In data rows 1 to 4 there was no significant difference in the measured rate constants if the reaction was carried out in the absence of NADH or complex I (CI), or if an inhibitor was added (rotenone 2.3 μM or piericidin A 0.25 μM). The rate constants for the reactions between DQ and Q_2H_2 and DQH_2 and Q_2 do not differ significantly, but the exchange reaction is faster in bovine phospholipids than in asolectin. In data rows 5 to 8 all the components of the assay are present and complex I is inhibited by either rotenone (2.3 or 11.5 μM) or piericidin A (0.25 or 1.25 μM). The rate constant does not depend on which inhibitor is present, on which combination of quinones is investigated, or on whether the reaction is carried out in bovine phospholipids or asolectin. All values are reported ± their 95 % confidence interval.

LEGENDS

Scheme 1. A). Schematic representation of complex I in the inner-mitochondrial membrane catalysing NADH oxidation, quinone reduction and proton translocation. B). Proposed Q-cycle mechanism of catalysis (reduction of two quinones and oxidation of one quinol for every NADH oxidised). Top: Q is reduced by one electron from the FeS chain (derived from NADH) and by one electron from quinol to form QH_2 and a semiquinone (right). Bottom: a second Q is reduced to form a second QH_2 and the SQ is oxidised to Q (left). Q: quinone; SQ: semiquinone; QH_2: quinol.

Scheme 2. Reaction schemes corresponding to the equations presented in Table 3. A). Reduction of a single quinone species (reaction rate determined by the reduction of Q, not the oxidation of NADH), inhibited competitively by quinol. B). The quinone:quinol self-exchange reaction. C). The inhibitor insensitive reduction of Q by complex I. D). The reaction scheme in A) expanded to describe the reduction of both DQ and Q_2, inhibited by both DQH_2 and Q_2H_2.

Figure 1. Experimental strategy aimed at detecting a Q-cycle in complex I. A). Complex I catalyses the simple reduction of quinone (Q) to quinol (QH_2), so that a different species of quinol (Q^*H_2) is unaffected and remains reduced throughout. B). Complex I catalyses a Q-cycle reaction (two quinones reduced and one quinol oxidised for every NADH oxidised), so that at the start of the reaction the oxidation of Q^*H_2 to Q* is observed. As the reaction progresses both Q* and Q are reduced to their corresponding quinols completely. Thus, detection of Q* is indicative of 'reductant-induced oxidation' and indicative of a Q-cycle mechanism. (+, concentration of NADH).

Figure 2. HPLC analysis of a mixture of the four quinone species. 20 μl of a mixture containing DQ (2.2 μM), DQH_2 (4.1 μM), Q_2 (3.2 μM) and Q_2H_2 (5.8 μM) was loaded onto a Nucleosil C18 column and eluted using a mobile phase of 50 mM sodium perchlorate in 53:25:22:0.1 v/v/v/v ethanol / water / methanol / 70 % perchloric acid (0.4 ml min^{-1}), and monitored at 290 nm (reported in milli-absorption units (mAU)). The four species elute at approximately 8.2 min. (Q_2H_2), 12.0 min. (Q_2), 14.5 min. (DQH_2) and 23.0 min. (DQ).

Figure 3. The reduction of DQ and Q_2 by NADH, catalysed by complex I. The reaction was initiated by the addition of approximately 100 μM DQ or Q_2 to assay buffer containing NADH, complex I and asolectin phospholipids, and monitored by HPLC analysis (◆ DQ, ■ Q_2, ◇ DQH_2, □ Q_2H_2) and UV-visible spectroscopy (+ NADH). A). Conversion of DQ to DQH_2 modelled using K_M = 24 μM , K_I = 26 μM and k_{cat} = 3.0 mol^{-1} dm^3 s^{-1}. B). Conversion of Q_2 to Q_2H_2 modelled using K_M = 20.4 μM , K_I = 15.7 μM and k_{cat} = 1.2 mol^{-1} dm^3 s^{-1}.

Figure 4. The self-exchange reaction of ubiquinone and ubiquinol. Different species of ubiquinone and ubiquinol were incubated together in the assay buffer at 30 °C, and their self-exchange reaction monitored over time by HPLC analysis (◆ DQ, ■ Q_2, ◇ DQH_2, □ Q_2H_2). A). DQ and Q_2H_2 incubated in the presence of complex I and bovine heart phospholipids, modelled using k_1 = 15 mol^{-1} dm^3 s^{-1}. B). DQ and Q_2H_2 incubated in the presence of NADH and asolectin, modelled using k_1 = 7 mol^{-1} dm^3 s^{-1}. C). DQH_2 and Q_2 incubated in the presence of complex I and asolectin, modelled using k_1 = 8 mol^{-1} dm^3 s^{-1}.

Figure 5. The self-exchange reaction of ubiquinone and ubiquinol in the presence of inhibited complex I. Different species of ubiquinone and ubiquinol were incubated together in the assay buffer at 30 °C, in the presence of complex I, phospholipids, NADH, and either rotenone or piericidin A, and their self-exchange reaction monitored over time by HPLC analysis (◆ DQ, ■ Q_2, ◇ DQH_2, □ Q_2H_2). A). DQ and Q_2H_2 in the presence of complex I inhibited by piericidin A (bovine phospholipids) modelled using k_1 = 52 mol^{-1} dm^3 s^{-1} (inhibitor-insensitive catalysis k_2 = 17 mol^{-1} dm^3 s^{-1}). B). DQH_2 and Q_2 incubated in the presence of complex I inhibited by rotenone (asolectin) modelled using k_1 = 65 mol^{-1} dm^3 s^{-1} (inhibitor insensitive catalysis k_2 = 44 mol^{-1} dm^3 s^{-1}). C). DQH_2 and Q_2 incubated in the presence of complex I inhibited by piericidin A (asolectin) modelled using k_1 = 77 mol^{-1} dm^3 s^{-1} (inhibitor insensitive catalysis k_2 = 33 mol^{-1} dm^3 s^{-1}).

Figure 6. The reduction of a quinone by complex I, in the presence of a different species of quinol. The quinone and quinol (DQ and Q_2H_2 (A) or Q_2 and DQH_2 (B)) were added to an assay buffer at 30 °C, containing complex I, phospholipids (asolectin) and NADH, and the reaction was

monitored over time by HPLC analysis (◆ DQ, ■ Q_2, ◇ DQH_2, □ Q_2H_2) and UV-visible spectroscopy (+ NADH). The points belonging to different data sets are joined for simplicity (the lines are not from data modelling).

Figure 7. The reduction of a quinone by complex I, in the presence of a different species of quinol, modelled using the change in NADH concentration. The quinone and quinol (DQ and Q_2H_2 (A) or Q_2 and DQH_2 (B)) were added to an assay buffer at 30 °C, containing complex I, phospholipids (asolectin) and NADH, and the reaction was monitored over time by HPLC analysis (◆ DQ, ■ Q_2, ◇ DQH_2, □ Q_2H_2, data reproduced from Figure 6). The modelled values were calculated using the change in NADH concentration (smoothed data derived from that shown in Figure 6) and the 'chance encounter' model (see text) with self-exchange rate constants of 44 mol^{-1} dm^3 s^{-1} (A) and 75 mol^{-1} dm^3 s^{-1} (B).

Scheme 1.

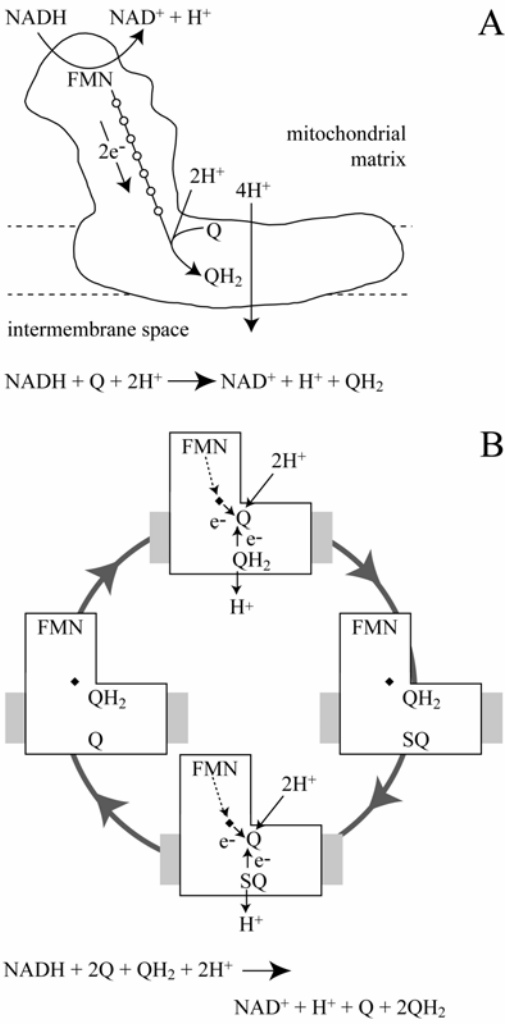

Scheme 2.

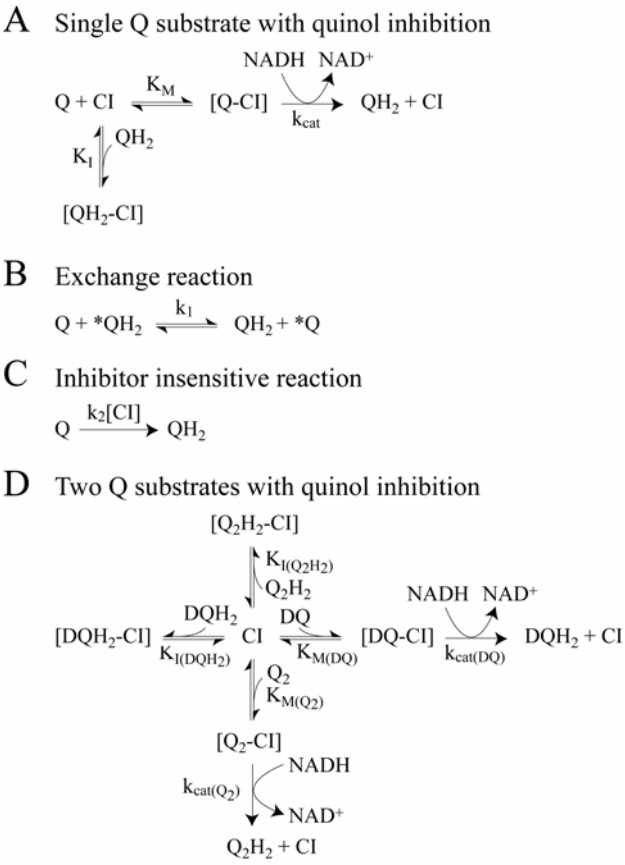

Figure 1

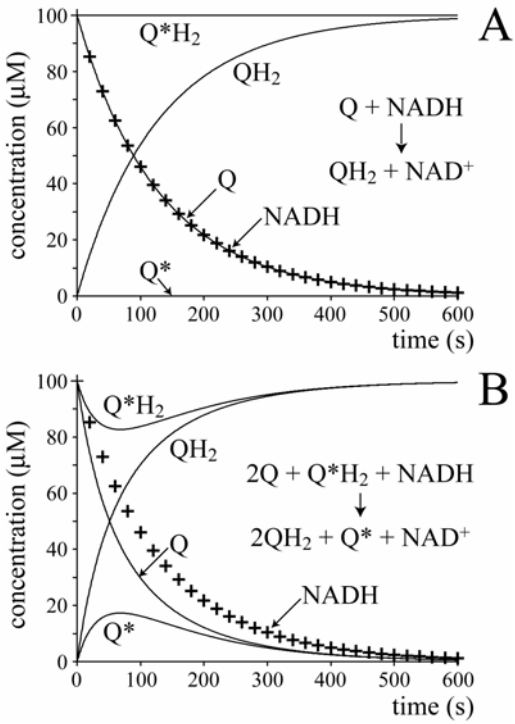

Figure 2

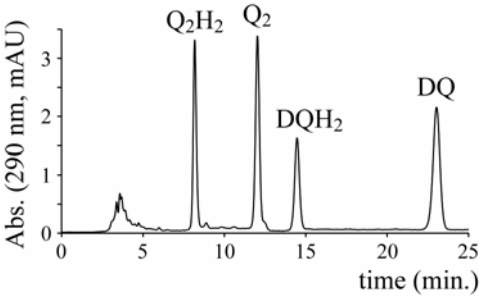

Figure 3

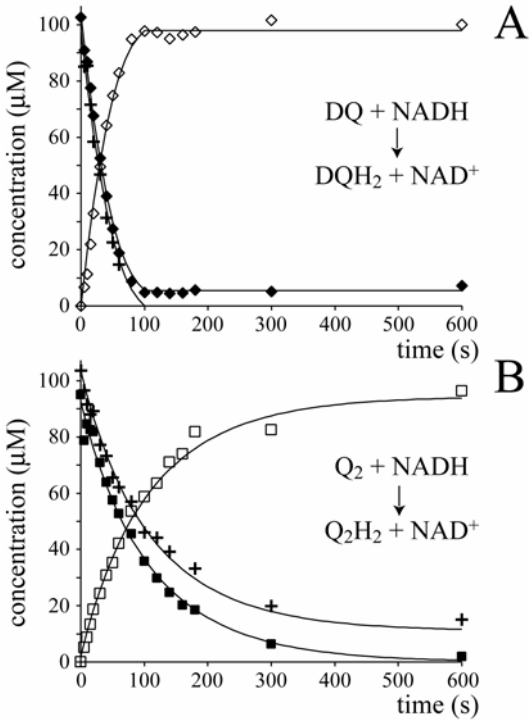

Figure 4

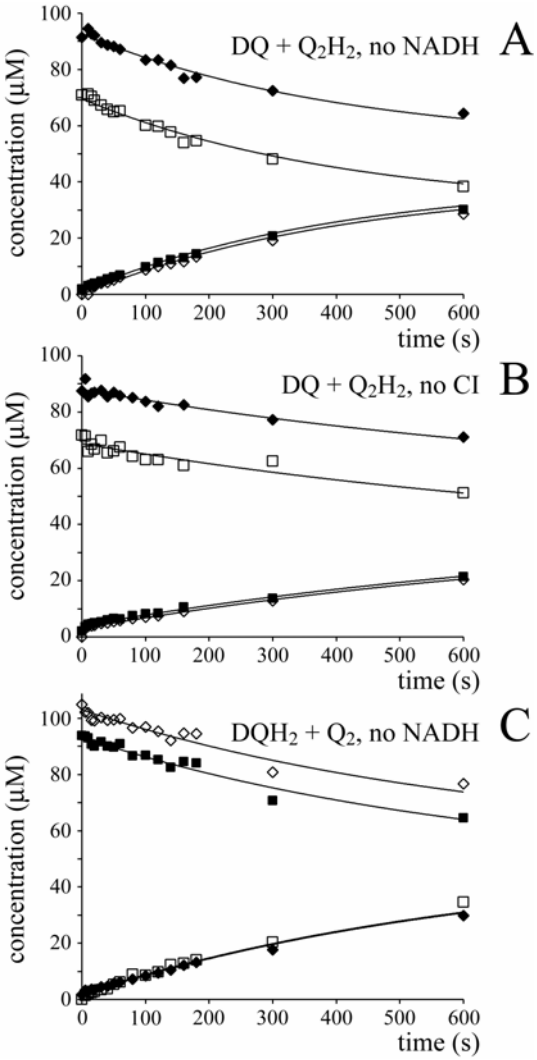

Figure 5.

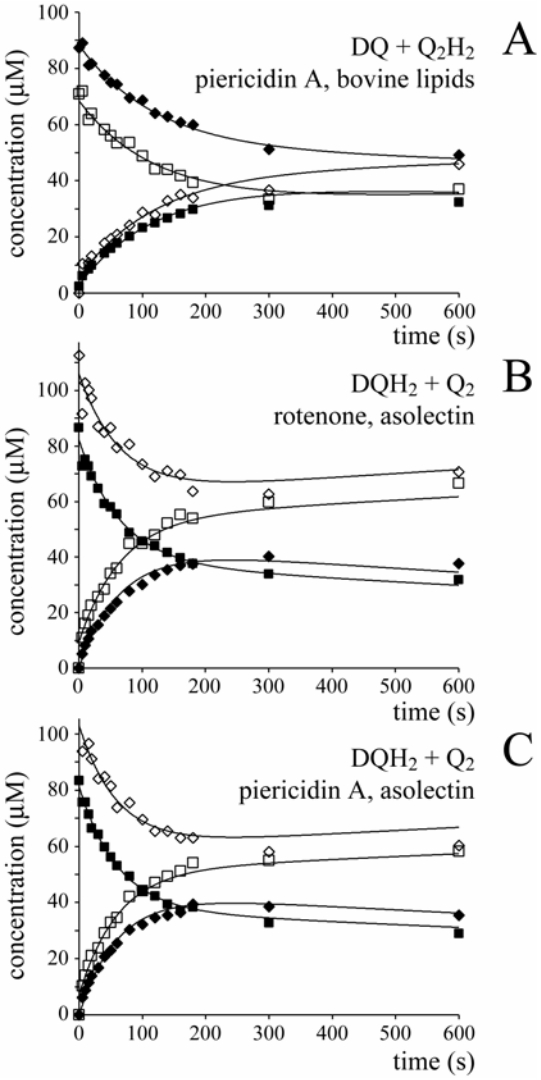

Figure 6.

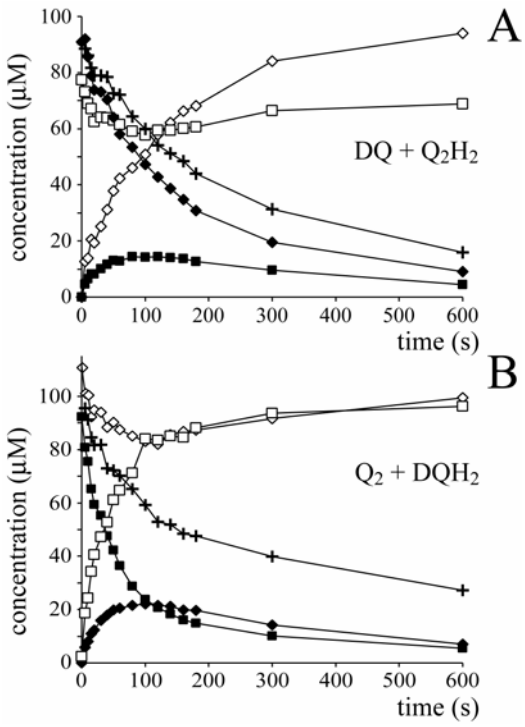

Figure 7.